SUPPORTING INFORMATION

Copper(I)/triphenylphosphine complexes containing naphthoquinone ligands as potential anticancer agents

Celisnolia M. Leite[1,2*], João Honorato de Araujo-Neto[3], Adriana P. M. Guedes[1], Analu R. Costa[1,2], Felipe C. Demidoff[4], Chaquip D. Netto[4], Eduardo E. Castellano[2], Otaciro R. do Nascimento[2], and Alzir A. Batista[1*]

1 Departamento de Química, Universidade Federal de São Carlos, CEP 13565-905, São Carlos, SP, Brazil
2 Instituto de Física de São Carlos, Universidade de São Paulo, CEP 13560-970, São Carlos, SP, Brazil
3 Instituto de Química, Universidade de São Paulo, CEP 27930-560, São Paulo, SP, Brazil
4Instituto Multidisciplinar de Química, Universidade Federal do Rio de Janeiro, CEP 35400-000, Macaé, RJ, Brazil

*Correspondence: celisnolia@hotmail.com and daab@ufscar.br; Tel.: +55 16 3351-8285.

FIGURES

Figure S3. UV-vis spectra in DMSO/Culture medium 1:199 of the complexes 1, 2, 3, and 4 at different times.
Figure S4. Clonogenic survival of MDA-MB-231 cells treated with different concentrations of complex 4 for 48 h.

TABLES

Table S1. Crystal data and structure refinement parameters were obtained for complexes 1 and 2.
Table S2. Tentative assignment of the vibrational frequencies (cm^{-1}) of the ν(C1=O1 ν(C2-O2) and ν(C4=O3) stretches for the free and after coordinated naphthoquinone ligands, and the respective shifts (Δ) after coordination.
Table S3. Maximum absorption wavelength (λ, nm), molar absorptivity (ε, $mol^{-1}L\ cm^{-1}$), and tentative assignment of the bands of the ligands NQ1-NQ4 and their respective complexes 1-4 in acetonitrile solution.
Table S4. EPR parameters obtained from simulation of the experimental spectra of the DMPO-˙OOH and DMPO-˙OH adducts.
Table S5. EPR parameters were obtained from a simulation of the spectrum measured at 77K temperature (liquid N2), with four spectral components.

FIGURES

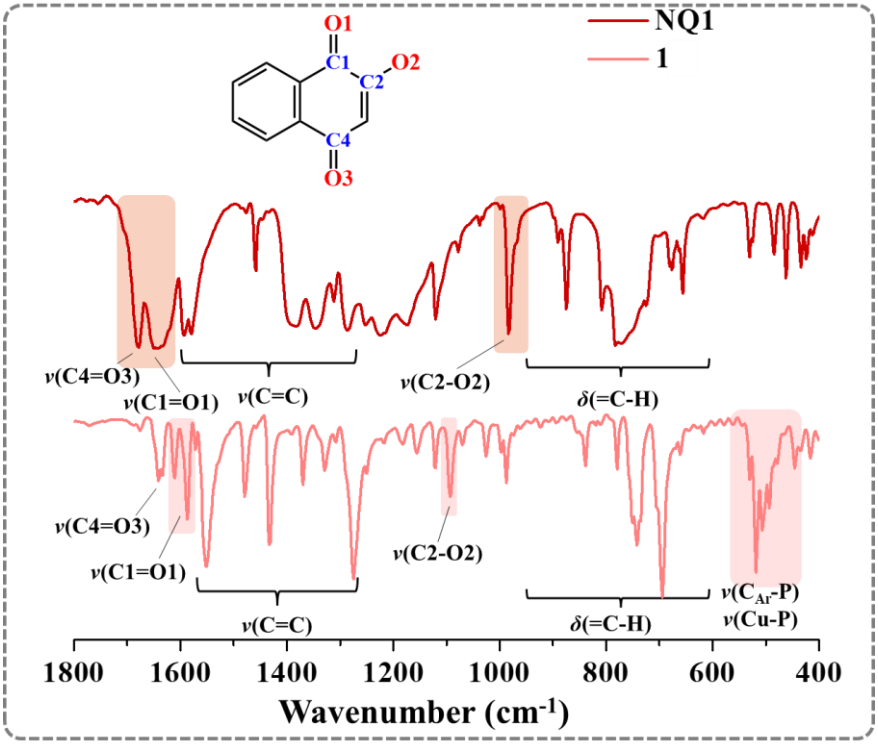

Figure S5. FTIR spectra for the Naphthoquinone ligand (NQ4) and Complex 1.

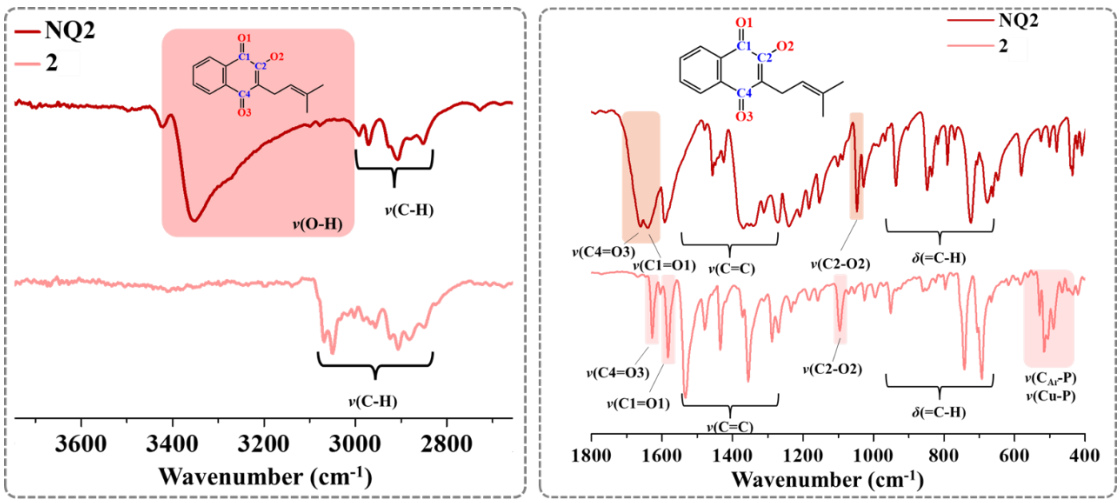

Figure S6. FTIR spectra for the Naphthoquinone ligand (NQ2) and Complex 2.

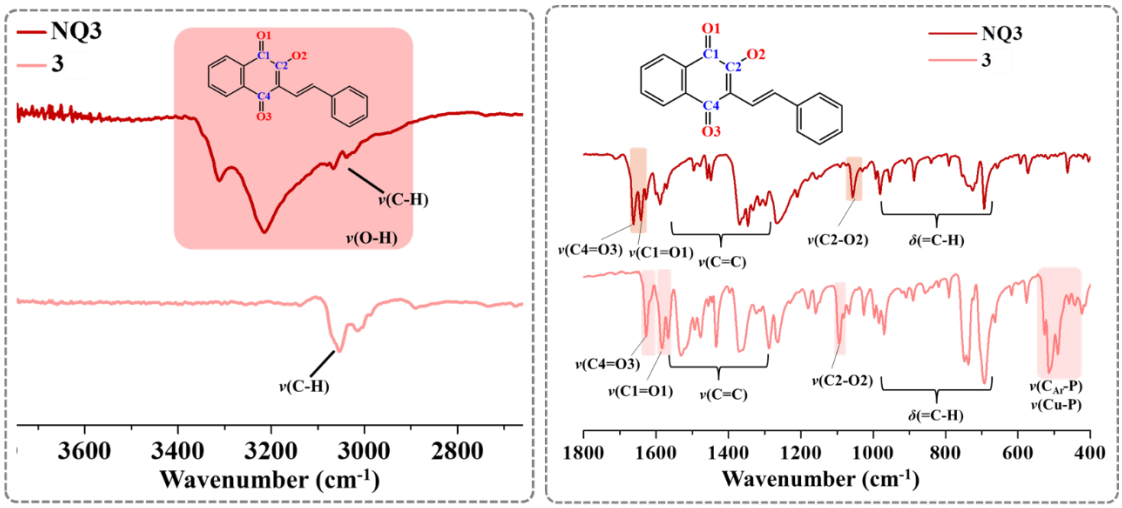

Figure S7. FTIR spectra for the Naphthoquinone ligand (NQ3) and Complex 3.

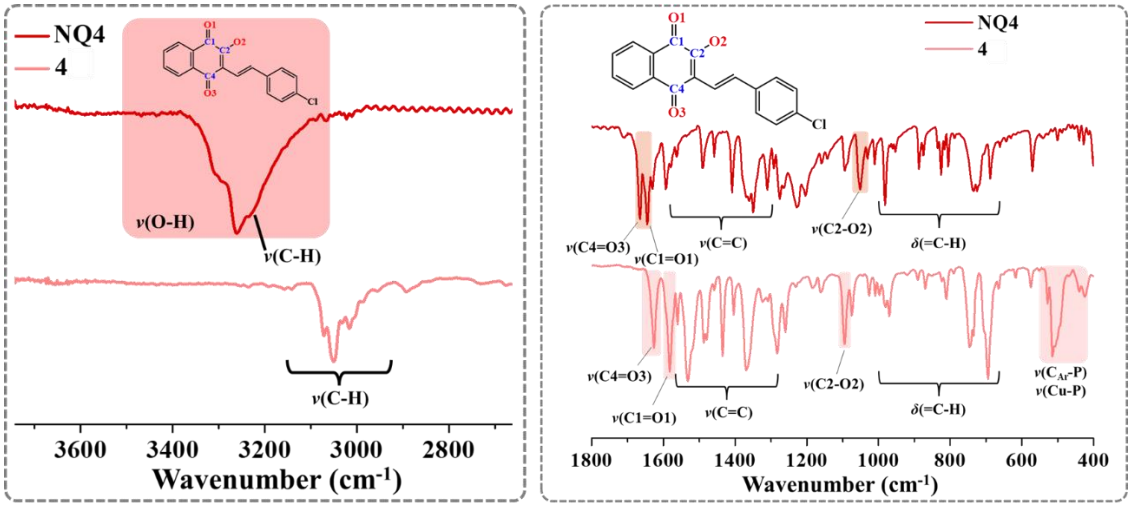

Figure S8. FTIR spectra for the Naphthoquinone ligand (NQ4) and Complex 4.

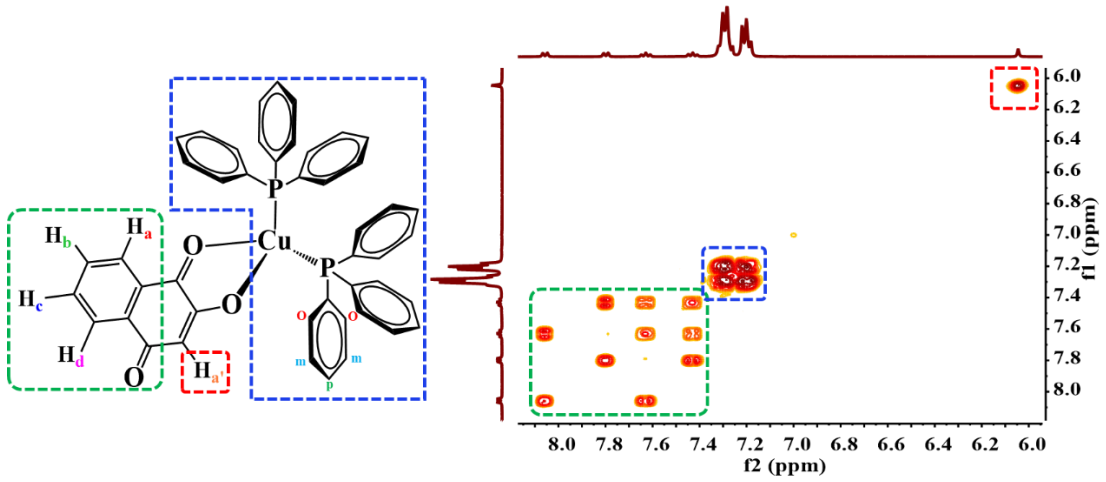

Figure S9. ^{1}H - ^{1}H COSY NMR of the aromatic region of Complex 1, in $CDCl_3$.

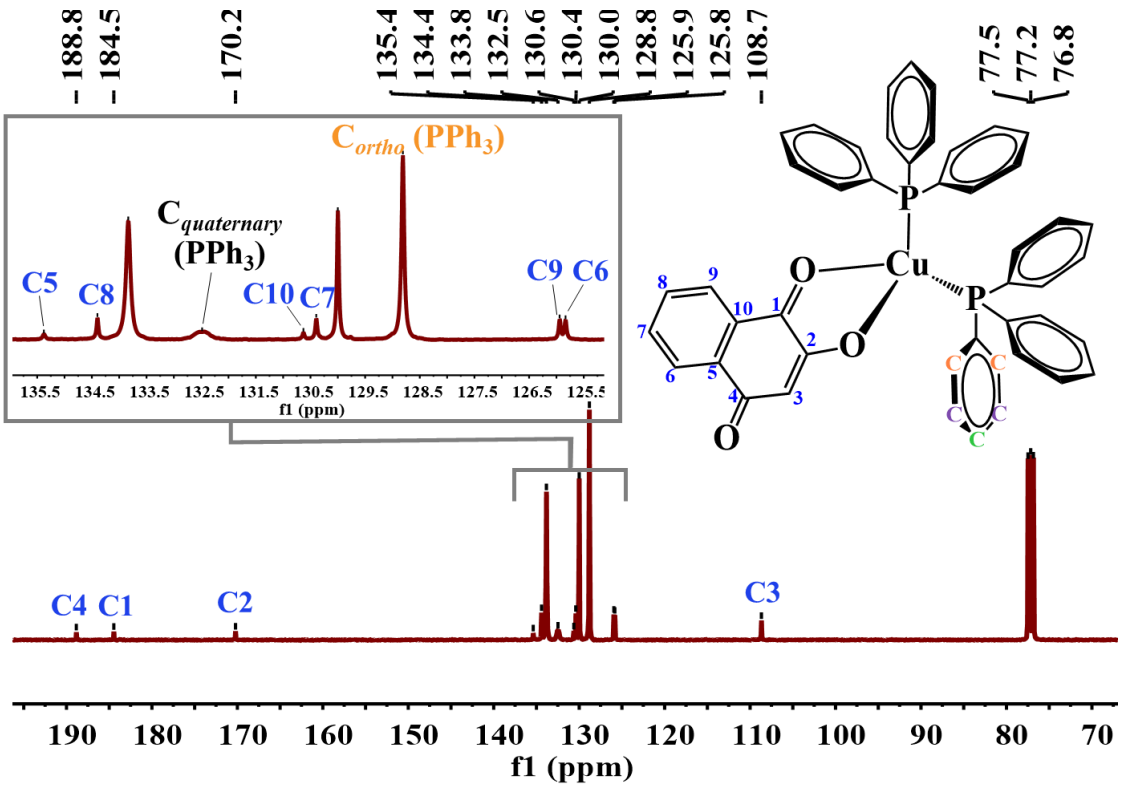

Figure S10. $^{13}C(^{1}H)$ NMR spectrum of Complex 1, in $CDCl_3$.

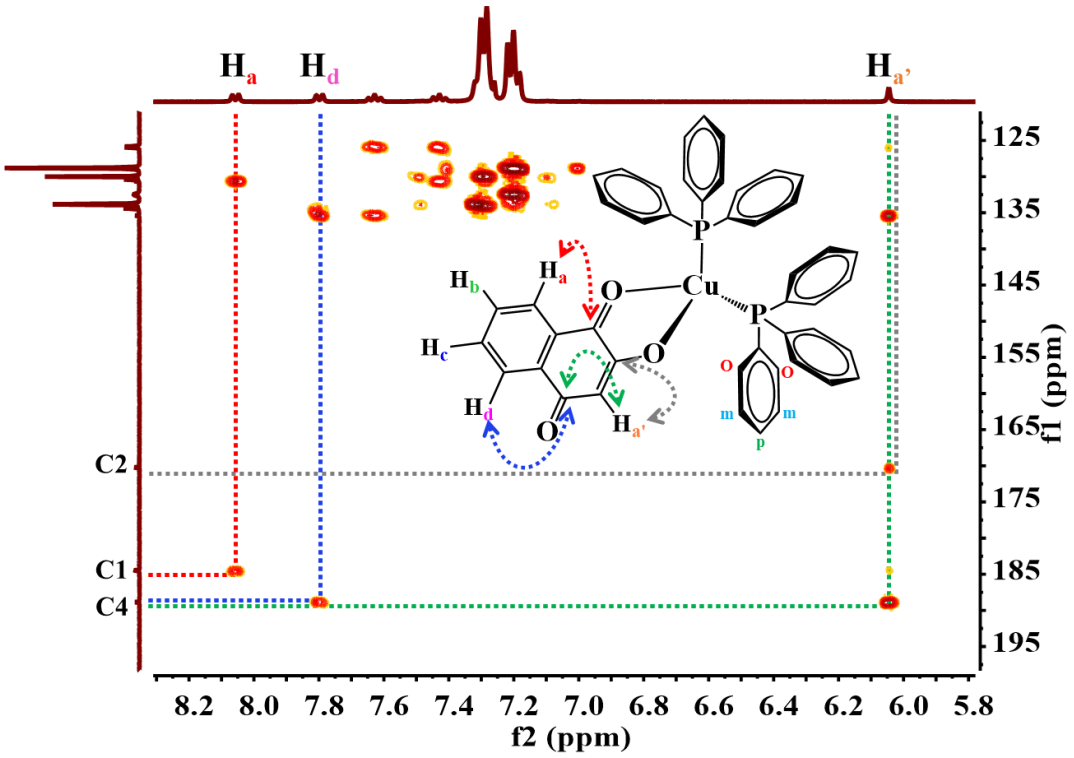

Figure S11. ^{1}H – ^{13}C HMBC NMR of Complex 1, in $CDCl_3$.

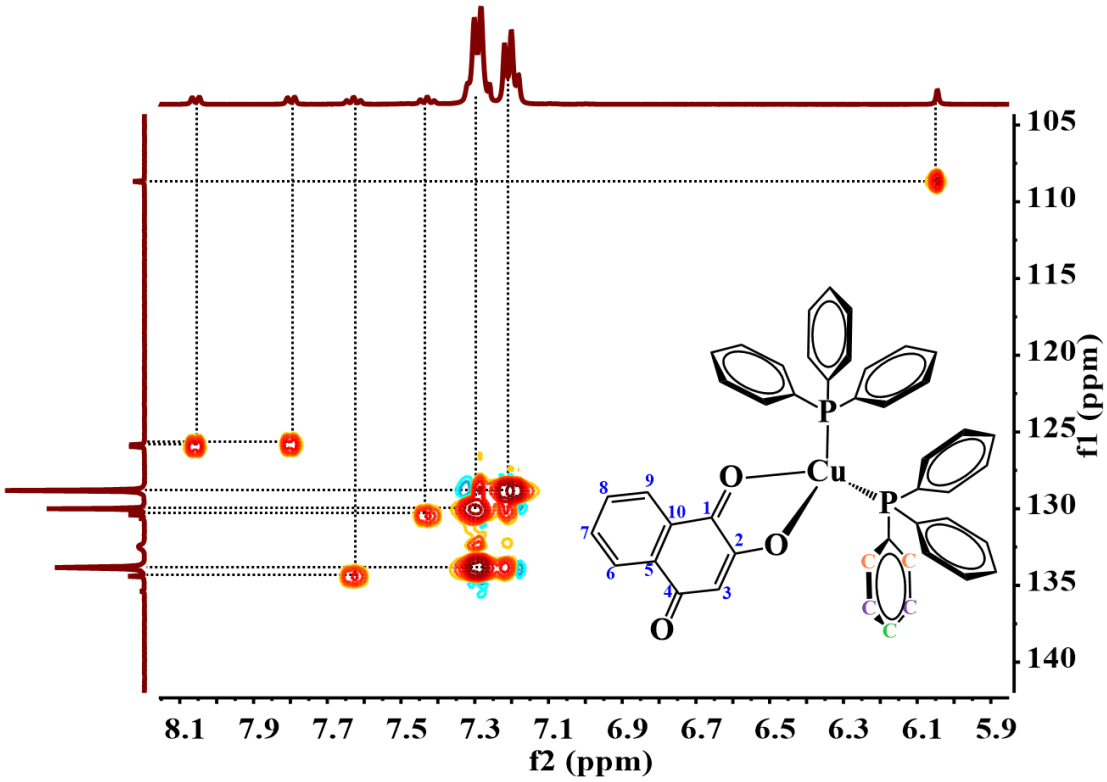

Figure S12. ^{1}H – ^{13}C HSQC NMR of Complex 1, in $CDCl_3$.

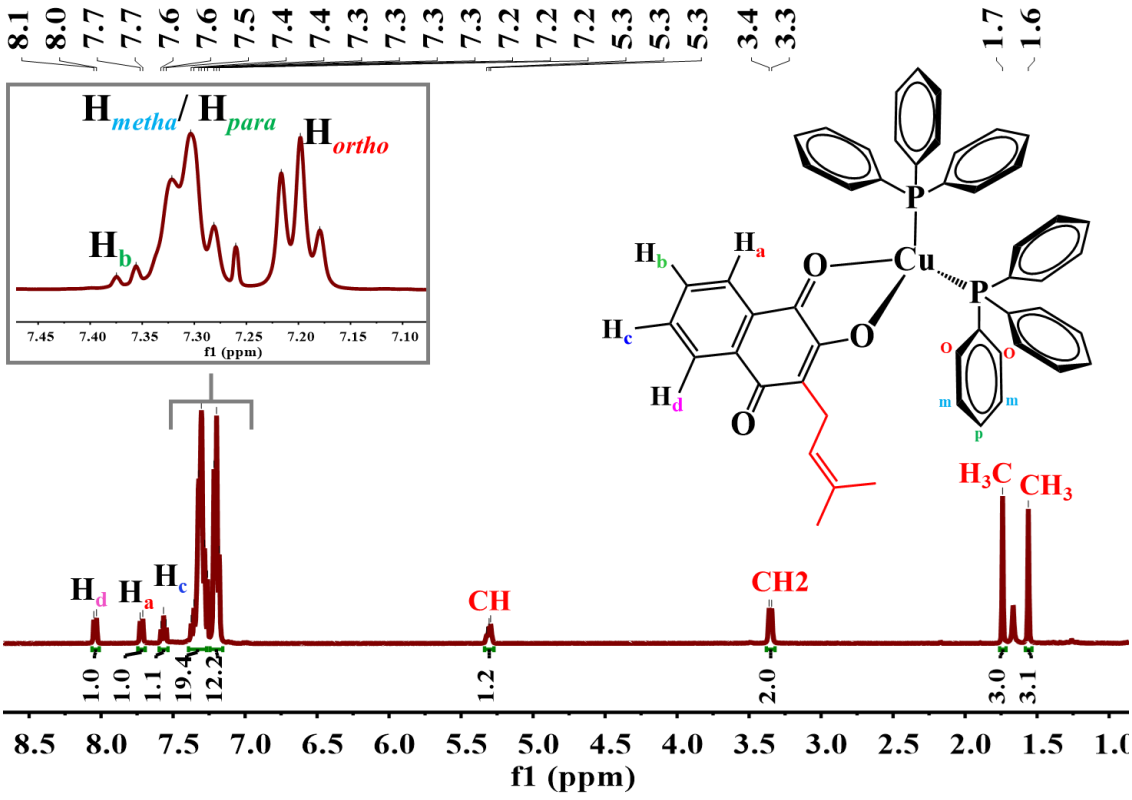

Figure S13. ^{1}H NMR spectrum of Complex 2, in $CDCl_3$.

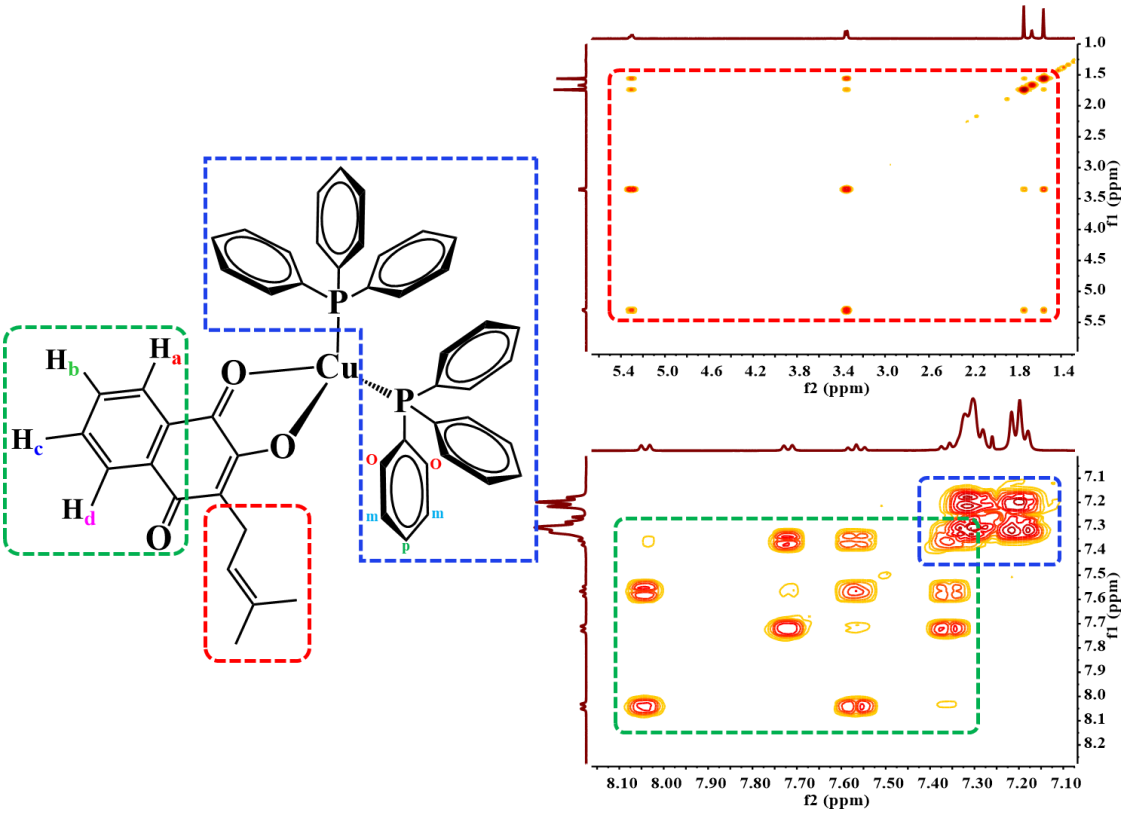

Figure S14. ^{1}H - ^{1}H COSY NMR of Complex 2, in $CDCl_3$.

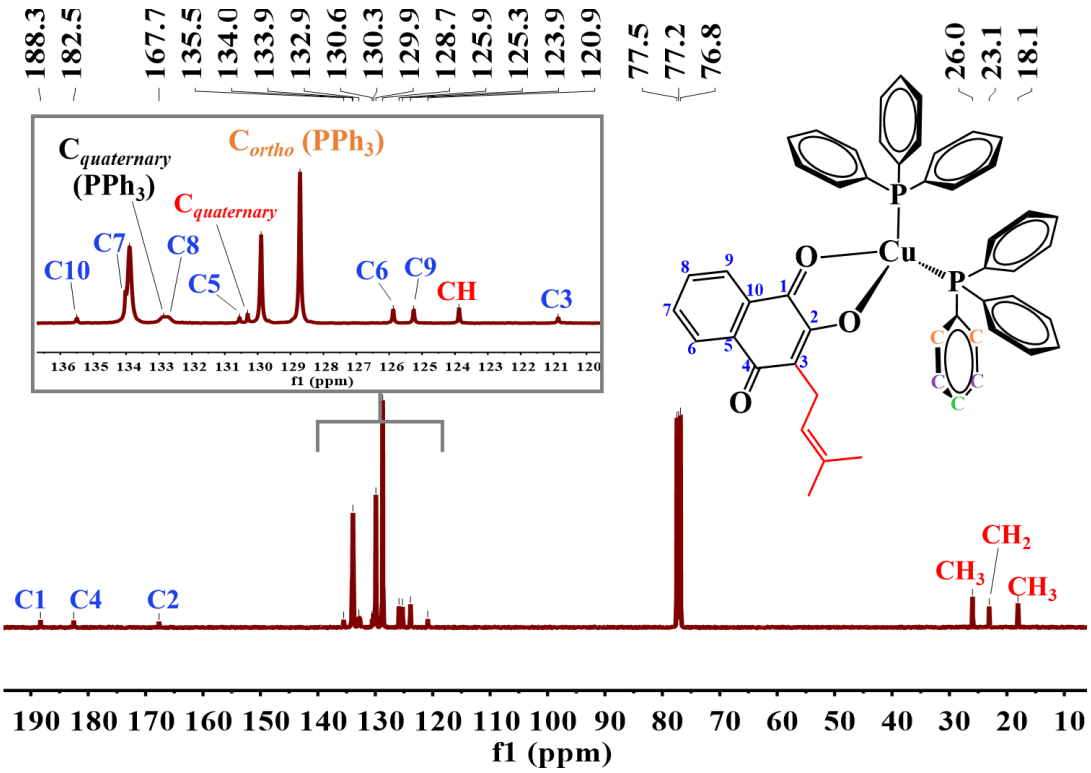

Figure S15. $^{13}C(^{1}H)$ NMR spectrum of Complex 2, in $CDCl_3$.

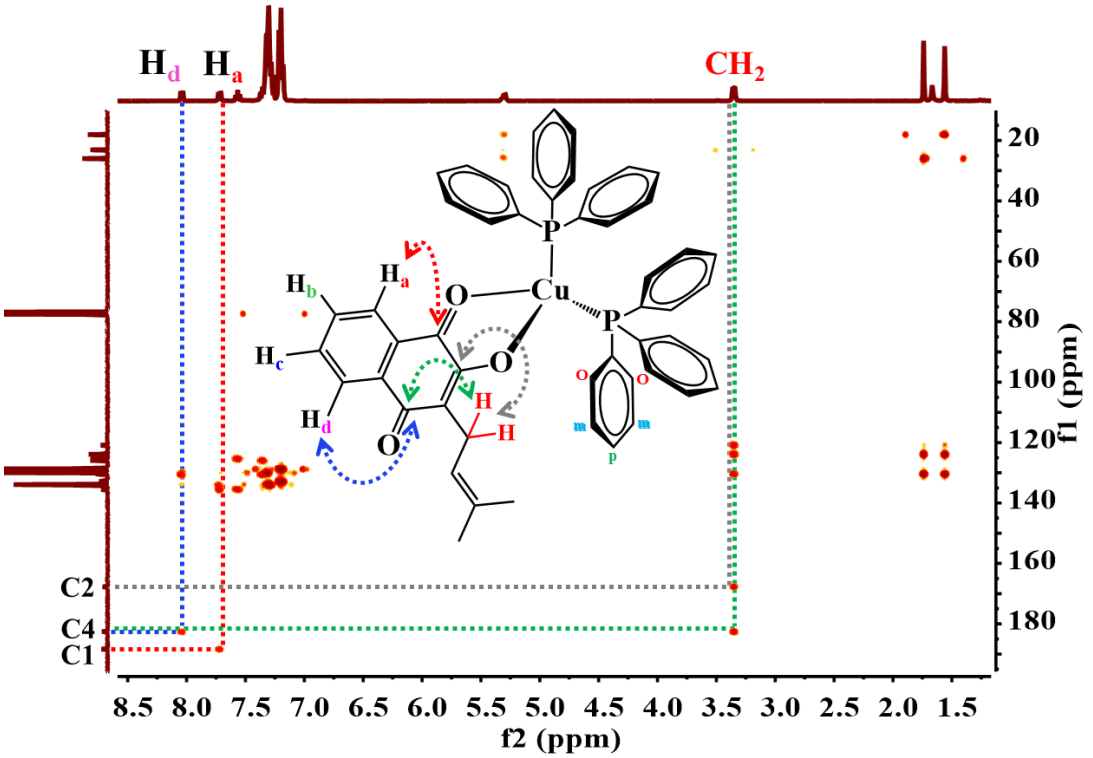

Figure S16. ^{1}H – ^{13}C HMBC NMR of Complex 2, in $CDCl_3$.

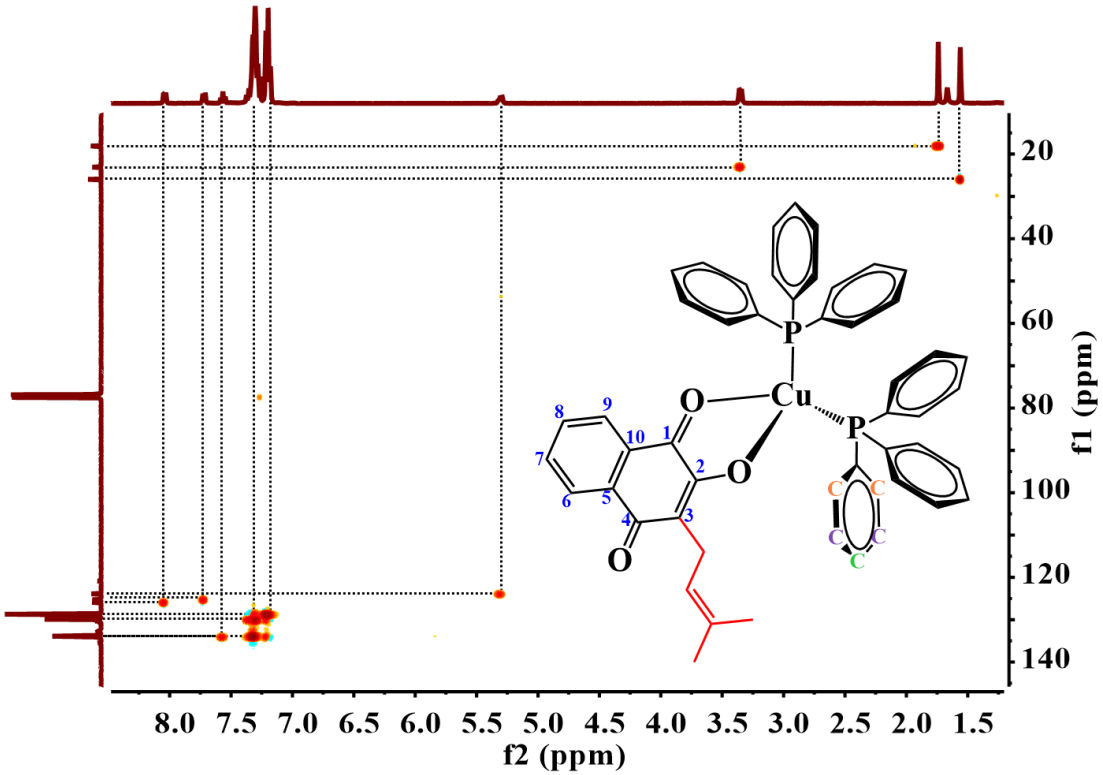

Figure S17. ^{1}H – ^{13}C HSQC NMR of Complex 2, in $CDCl_3$.

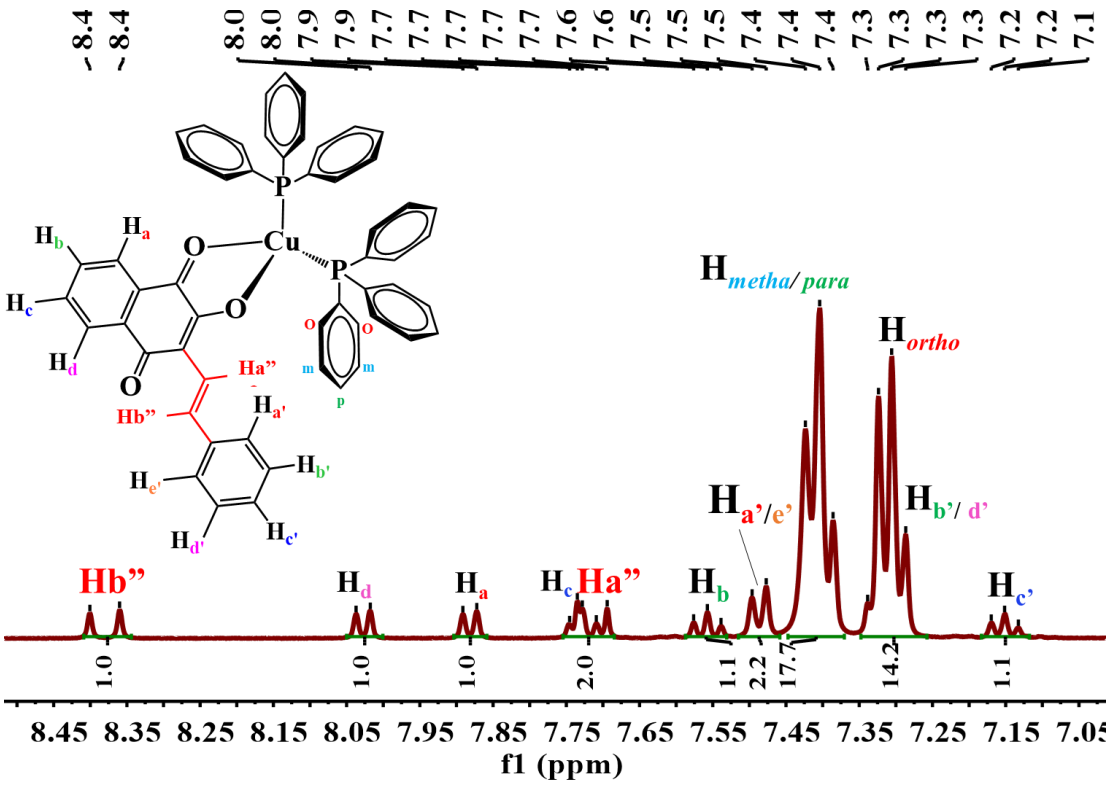

Figure S18. ^{1}H NMR spectrum of Complex 3, in $(CD_3)_2CO$.

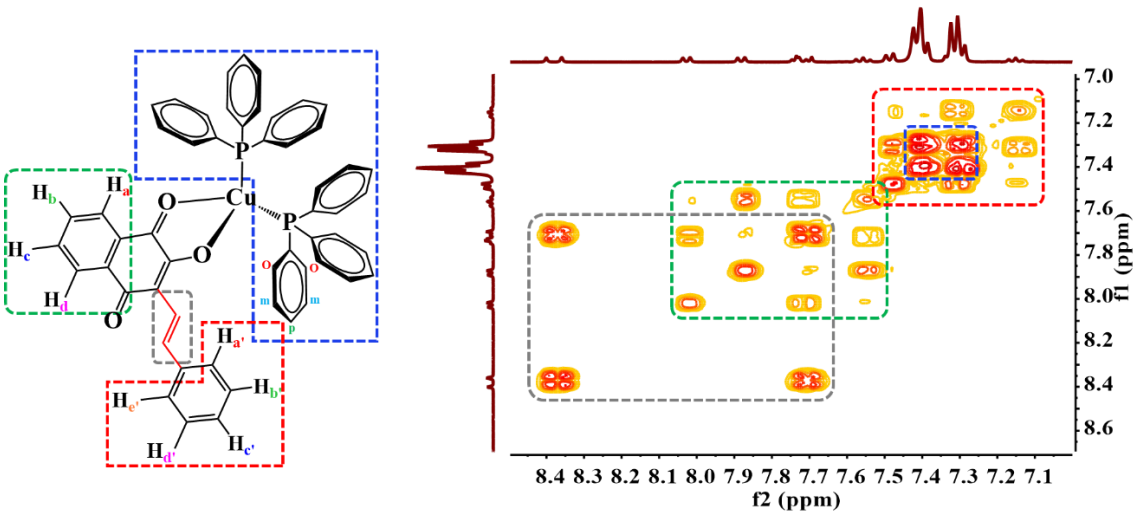

Figure S19. ^{1}H - ^{1}H COSY NMR of Complex 3, in $(CD_3)_2CO$.

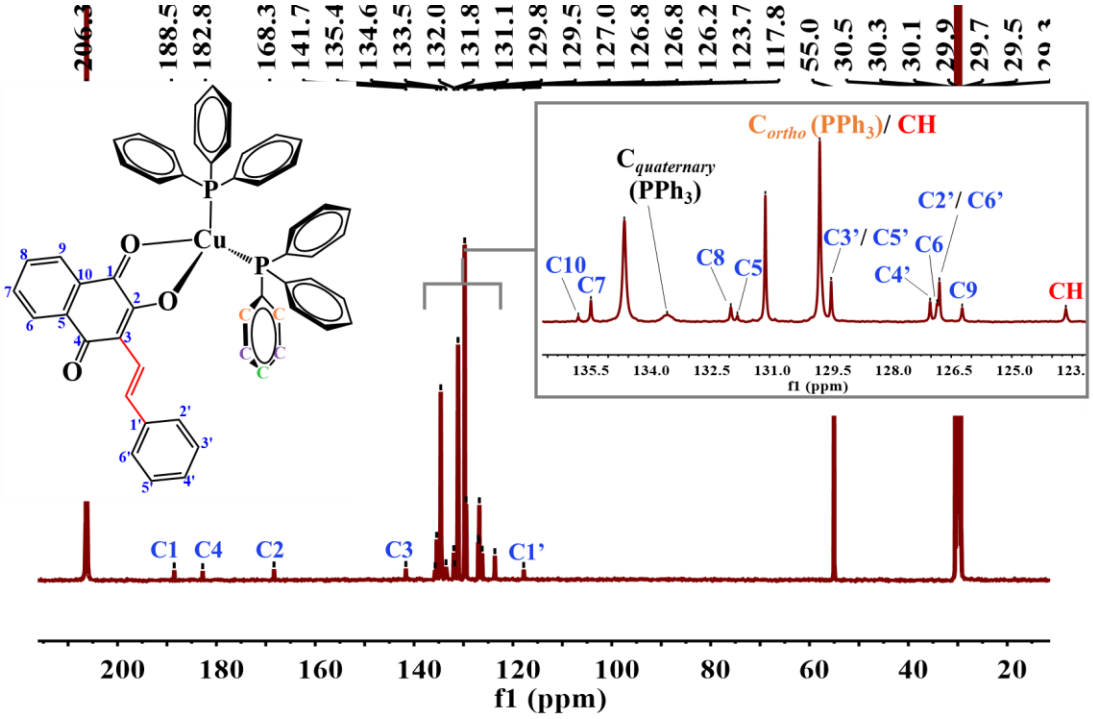

Figure S20. $^{13}C(^{1}H)$ NMR spectrum of Complex 3, in $(CD_3)_2CO$.

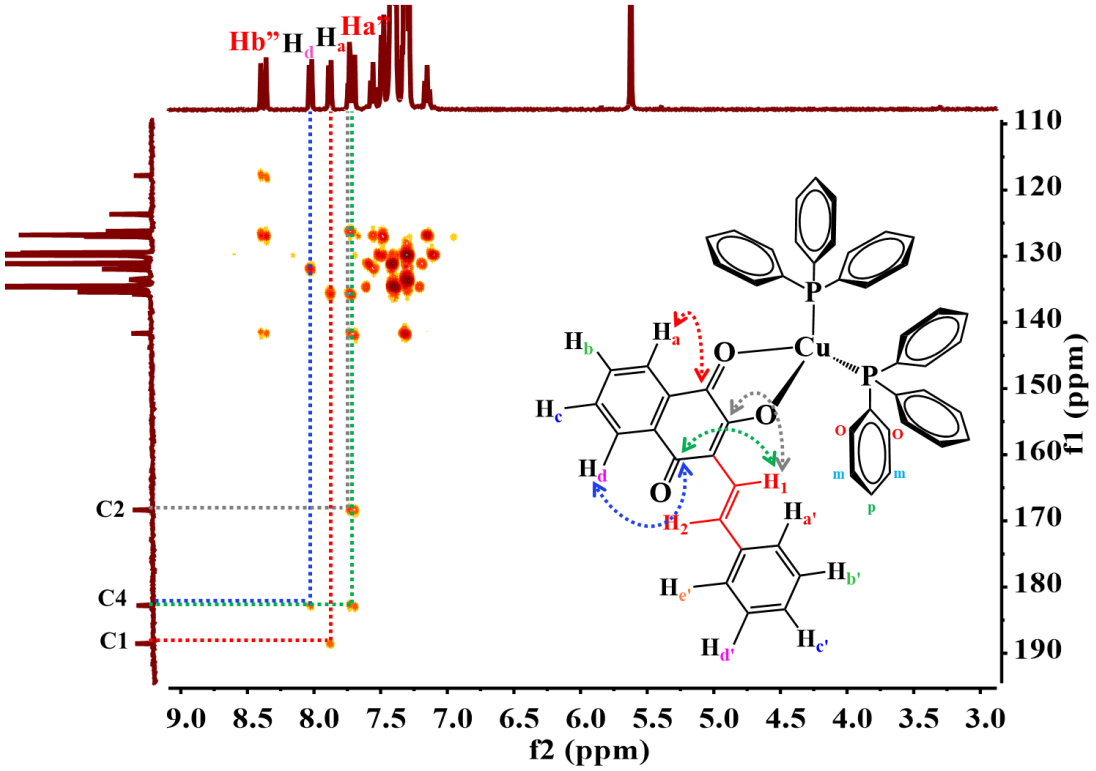

Figure S21. $^{1}H - ^{13}C$ HMBC NMR of Complex 3, in $(CD_3)_2CO$.

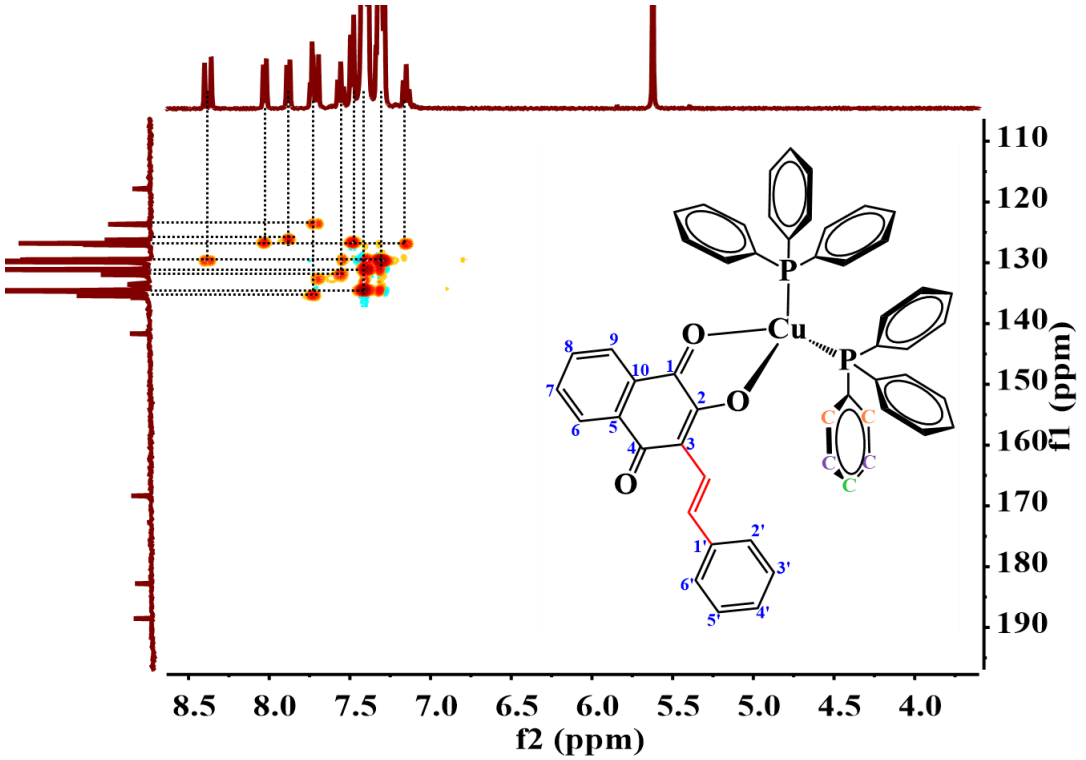

Figure S22. ^{1}H – ^{13}C HSQC NMR of Complex 3, in $(CD_3)_2CO$.

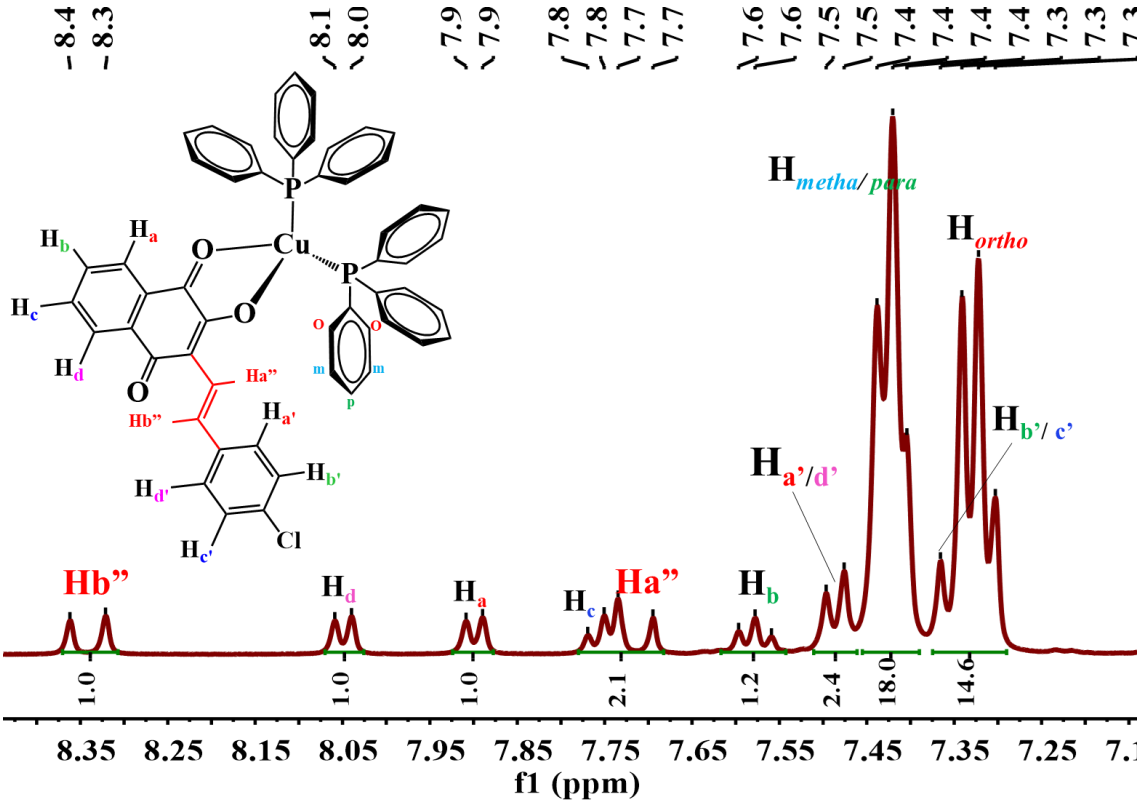

Figure S23. ^{1}H NMR spectrum of Complex 4, in $(CD_3)_2CO$.

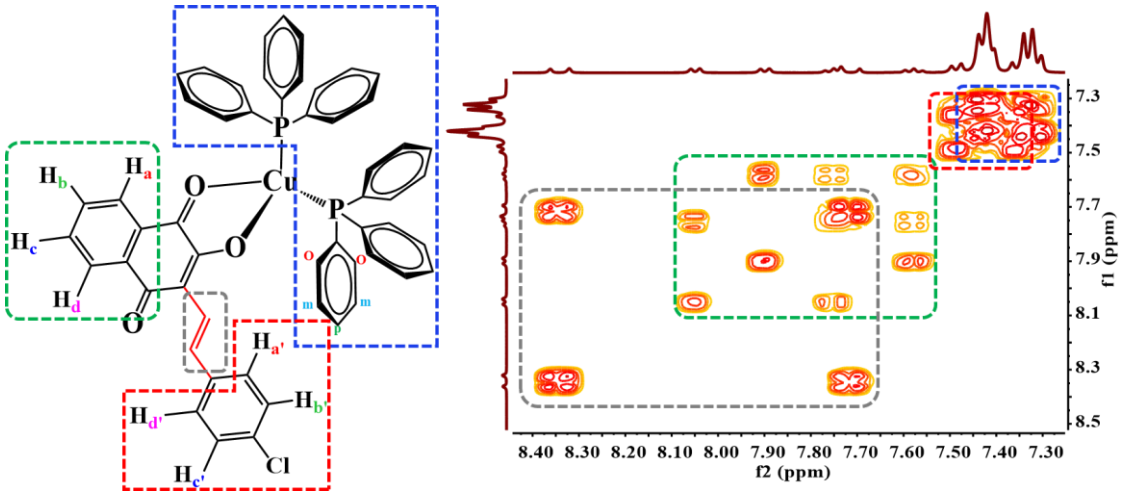

Figure S24. ^{1}H - ^{1}H COSY NMR of Complex 4, in $(CD_3)_2CO$.

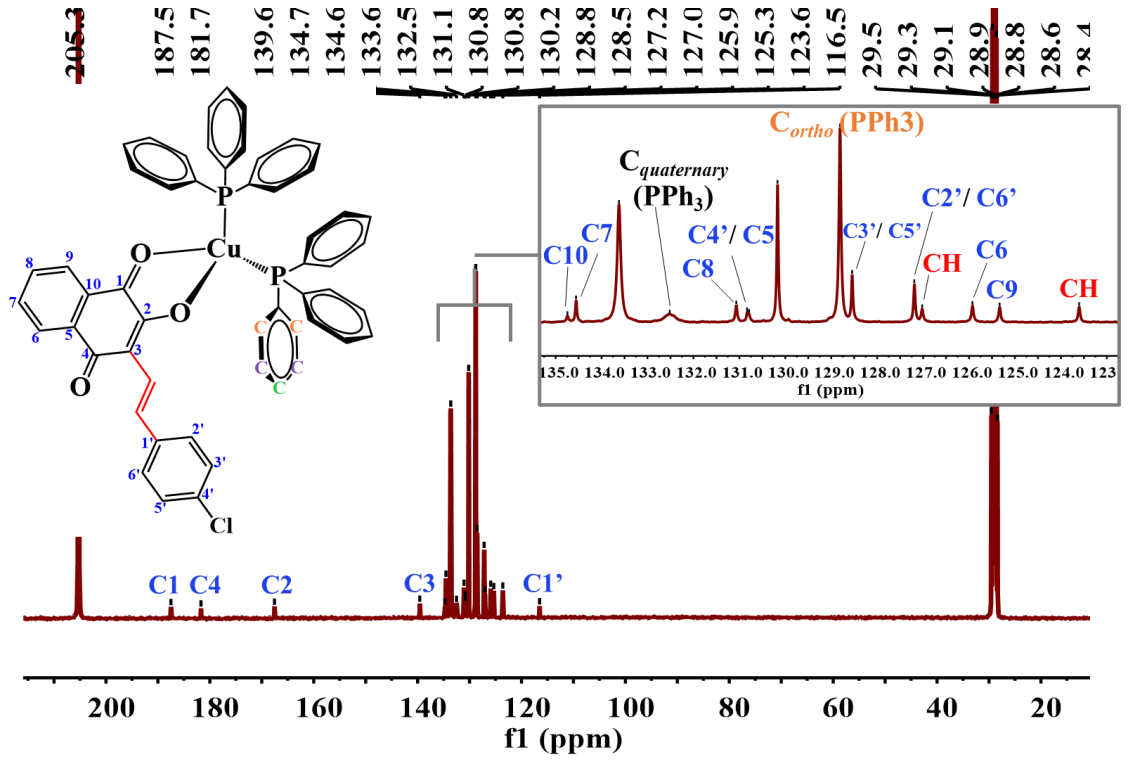

Figure S25. $^{13}C(^{1}H)$ NMR spectrum of Complex 4, in $(CD_3)_2CO$.

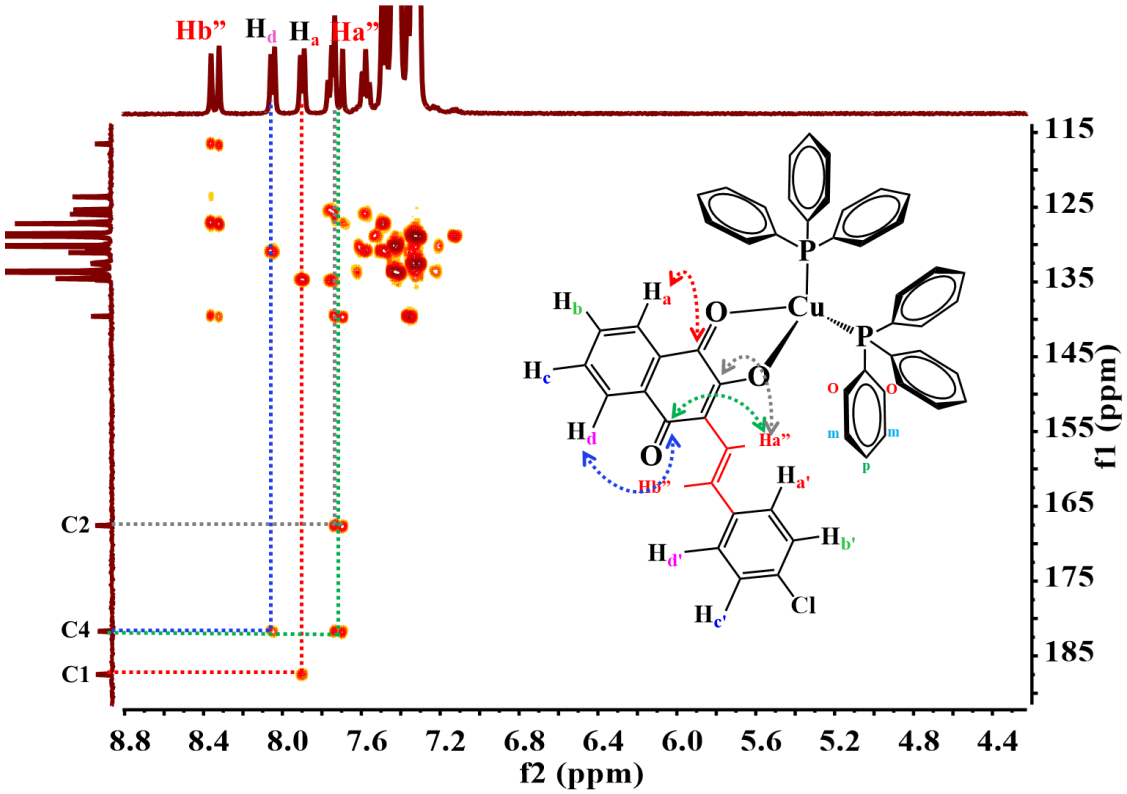

Figure S26. ^{1}H – ^{13}C HMBC NMR of Complex 4, in $(CD_3)_2CO$.

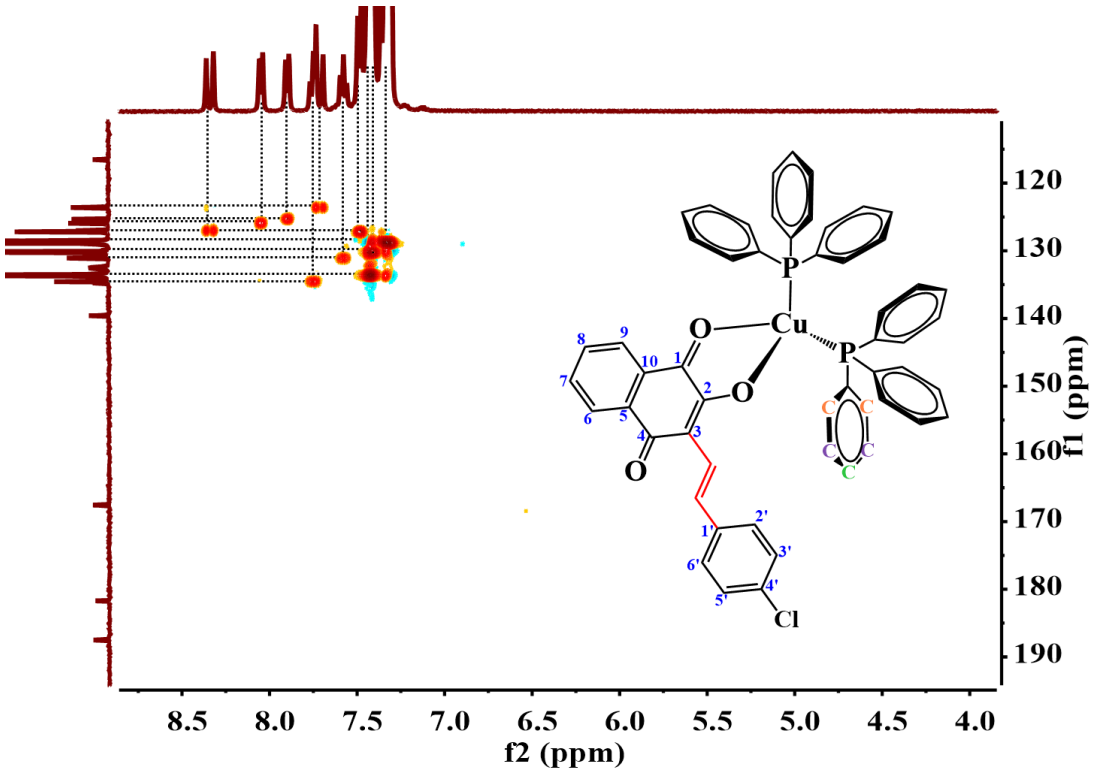

Figure S27. ^{1}H – ^{13}C HSQC NMR of Complex 4, in $(CD_3)_2CO$.

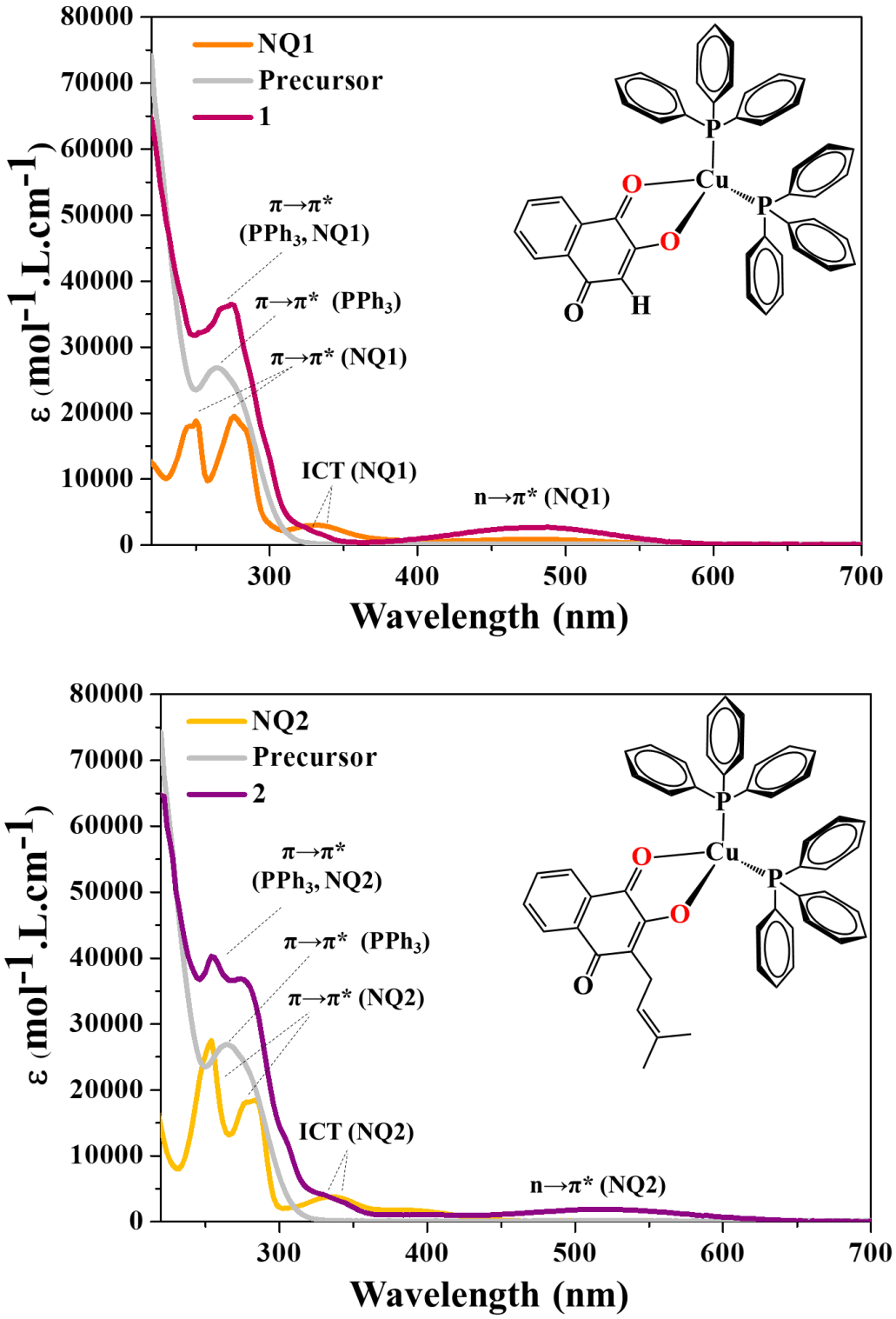

Figure S28. UV-vis absorbance for samples of the precursor complex, complexes 1 and 2, and their respective naphthoquinone ligands, in acetonitrile.

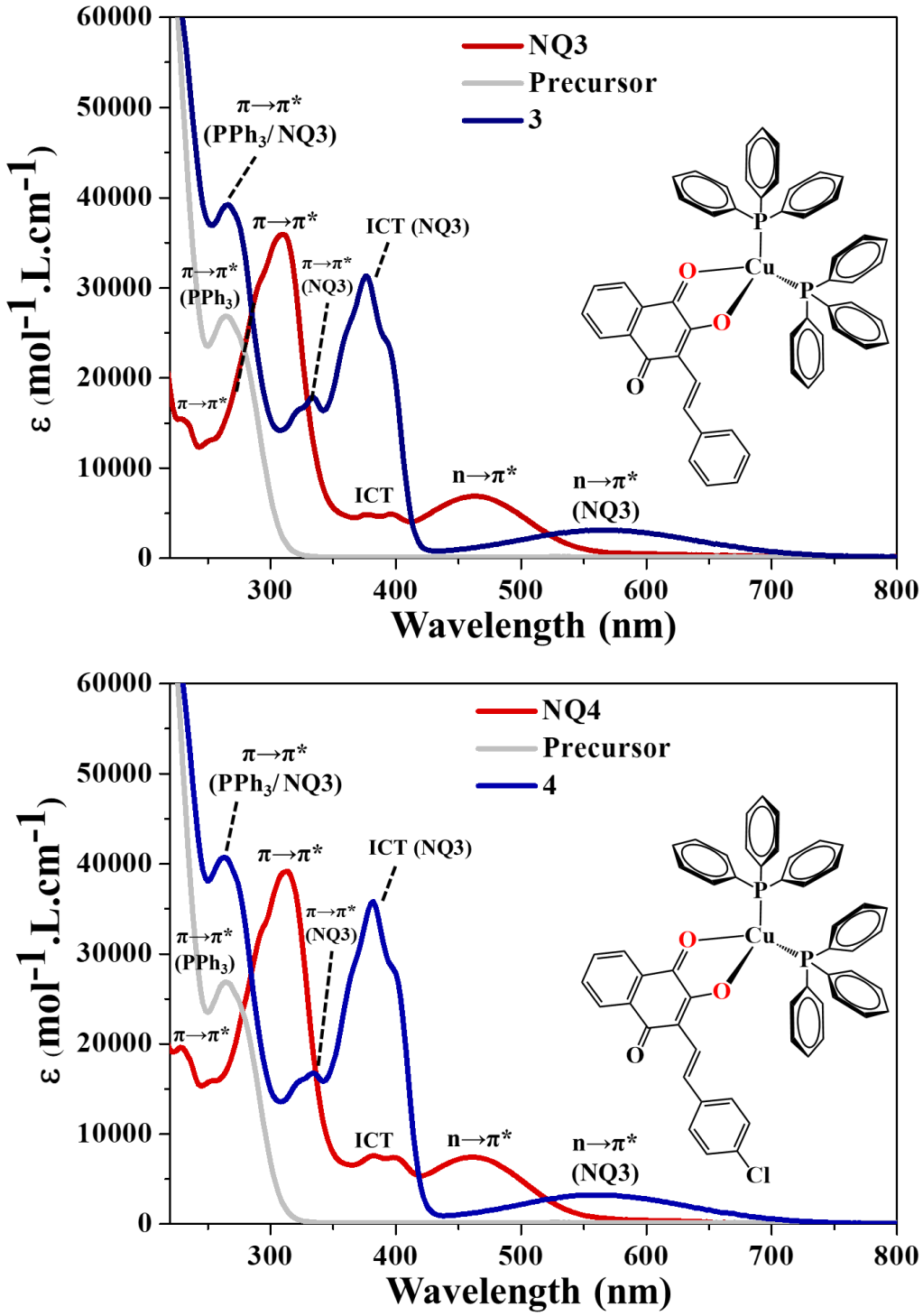

Figure S29. UV-vis absorbance for samples of the precursor complex, complexes 3 and 4, and their respective naphthoquinone ligands, in acetonitrile.

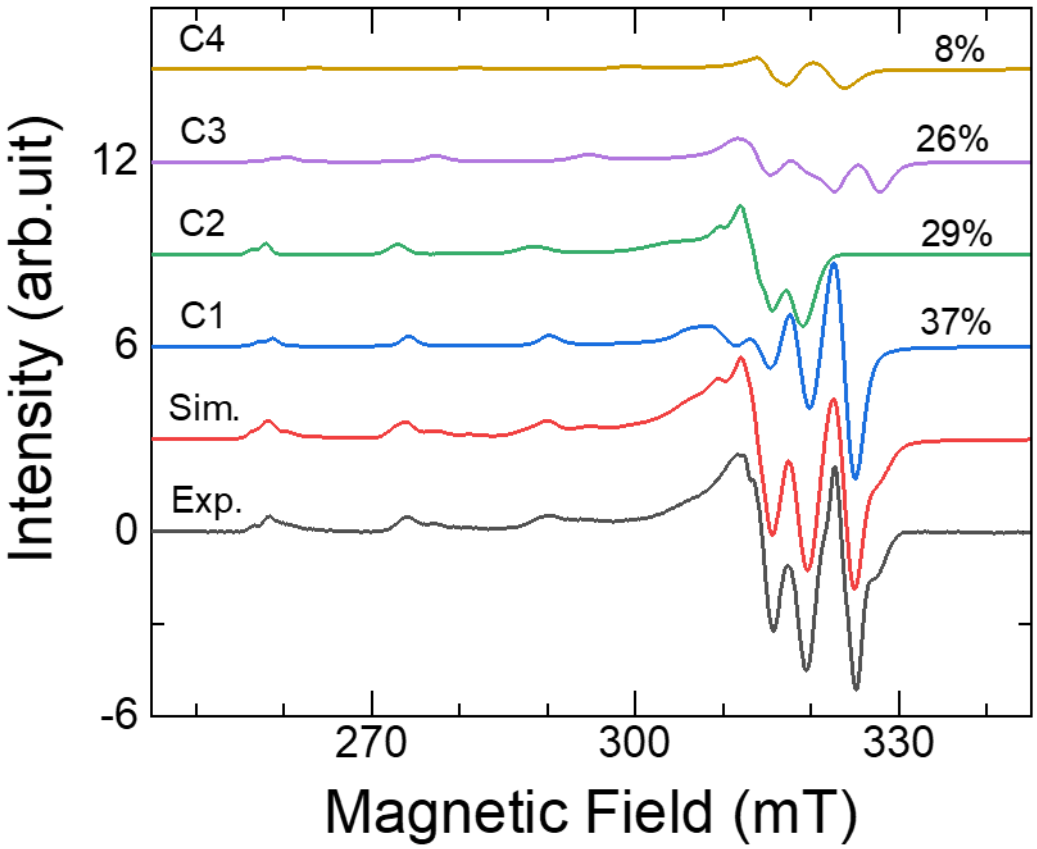

Figure S30. EPR spectra of Compound 4 reacted with DMPO in DMSO solvent at 77K. C1, C2, C3 and C4 are the components that result in the best fit of the experimental spectra. In the spectra of components C1 and C2, it was necessary to include the superhyperfin interaction of a nuclear spin nucleus I=1/2, compatible with a P (phosphorus) phosphine ligand. The spectra of the C3 and C4 components show no superhyperfine interactions suggesting interaction ligands with DMSO and the oxygens of the naphthoquinone. By calculating the areas obtained by double integration, it was possible to estimate the relative concentrations of each component to the experimental spectrum, namely, C1 37%, C2 29%, C3 26%, and C4 8%.

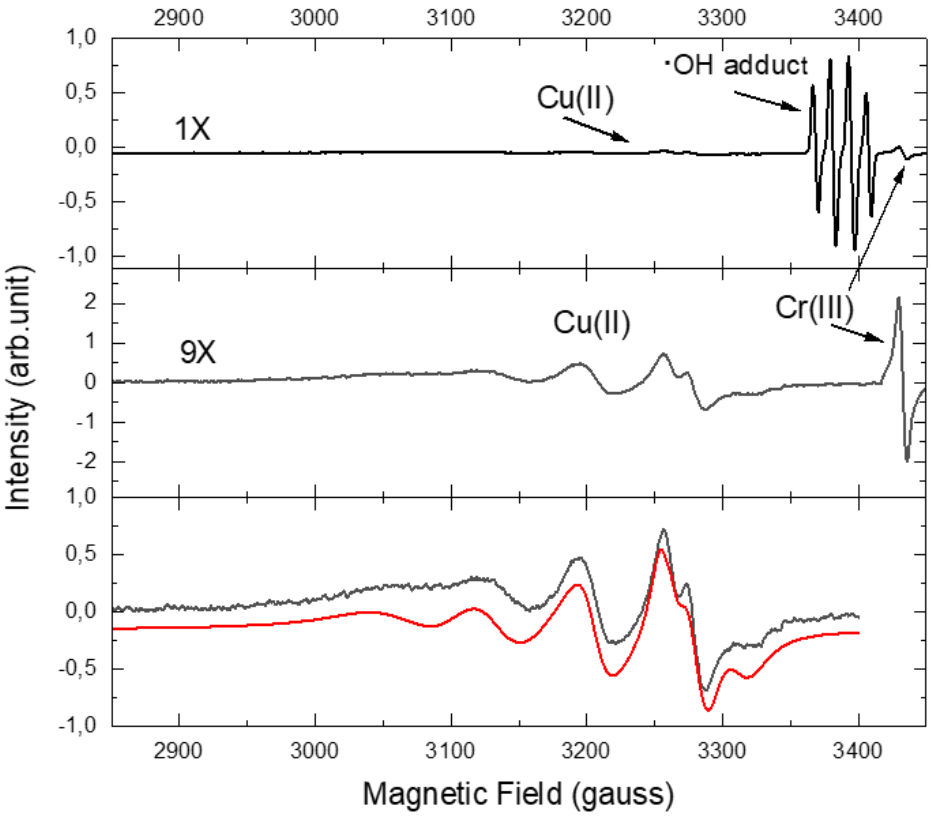

Figure S31. EPR spectra of compound 4b reacted with DMPO in DMSO solvent at room temperature. Layer superior is the complete spectra including Cu(II) compounds, DMPO adduct and Cr(III) marker (g=1.9797). Panel central is the Cu(II) and Cr(III) marker accumulated 9 times. Panel inferior is only the EPR spectra of Cu compounds scaled and the spectral simulation using EasySpin program with the four componentes.

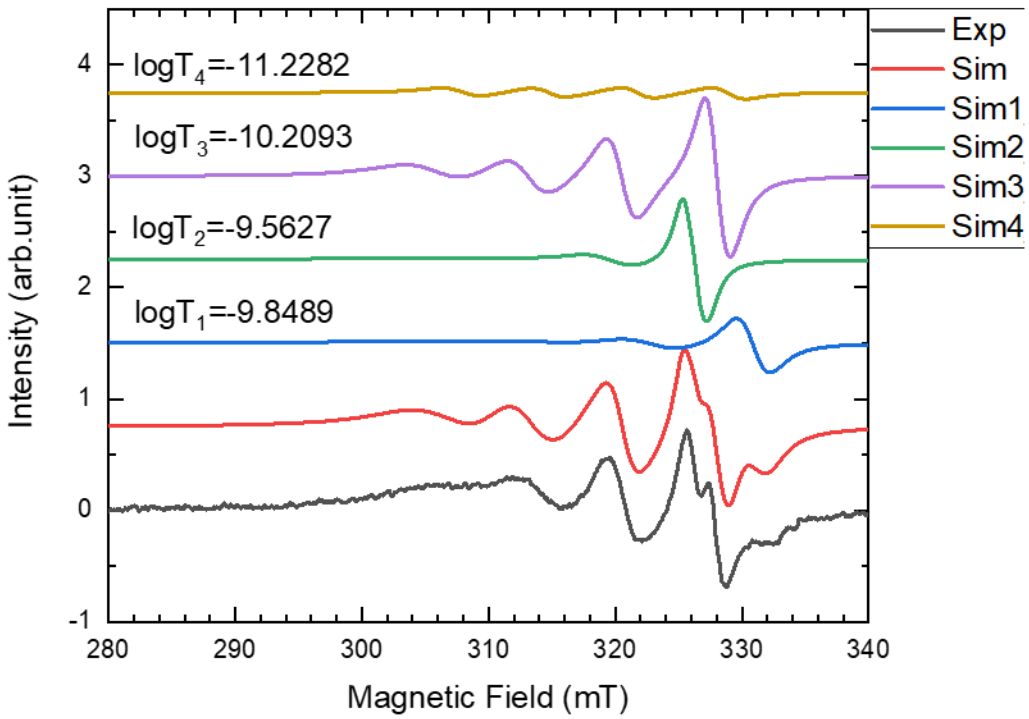

Figure S32. EPR spectra of Complex 4 reacted with DMPO in DMSO solvent at room temperature. Sim1, Sim2, Sim3 and Sim4 are the components that result in the best fit of the experimental spectra. The correlation time are indicated in each component. The values of the rotational correlation times, which is dependent on the size of the molecules, are consistent with the existence of two larger and two smaller molecules, indicating that the two larger ones contain a bound phosphine while the two smaller ones, the phosphines are replaced by molecules from the solvent and probably water.

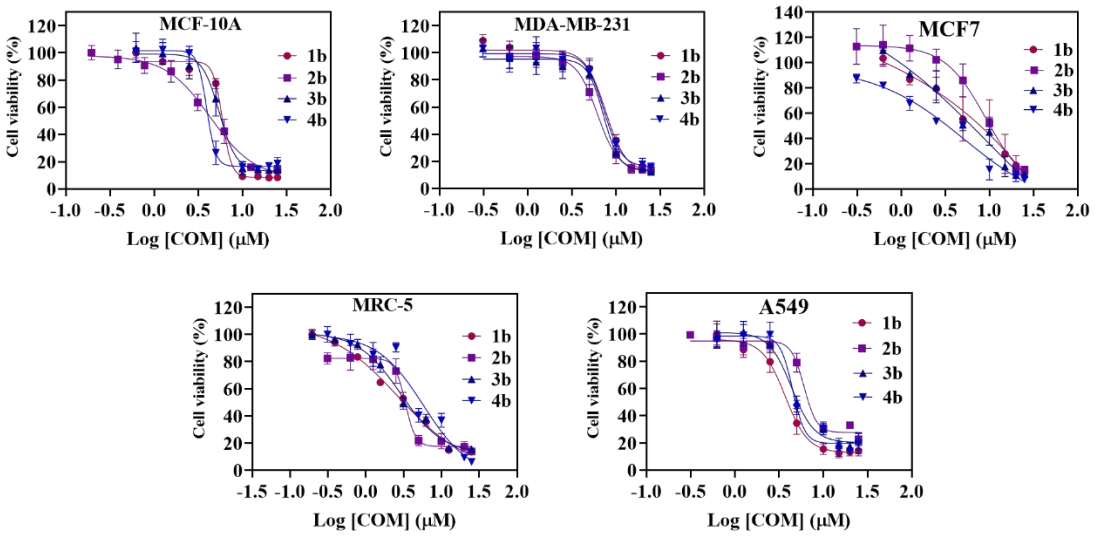

Figure S33. Cytotoxicity of complexes. Concentration-response curve of tumor cells (MDA-MB-231, MCF7 and A549) and non-tumor cells (MCF-10A and MRC-5) after complexes treatment (0.3 to 25 μM) for 48 h.

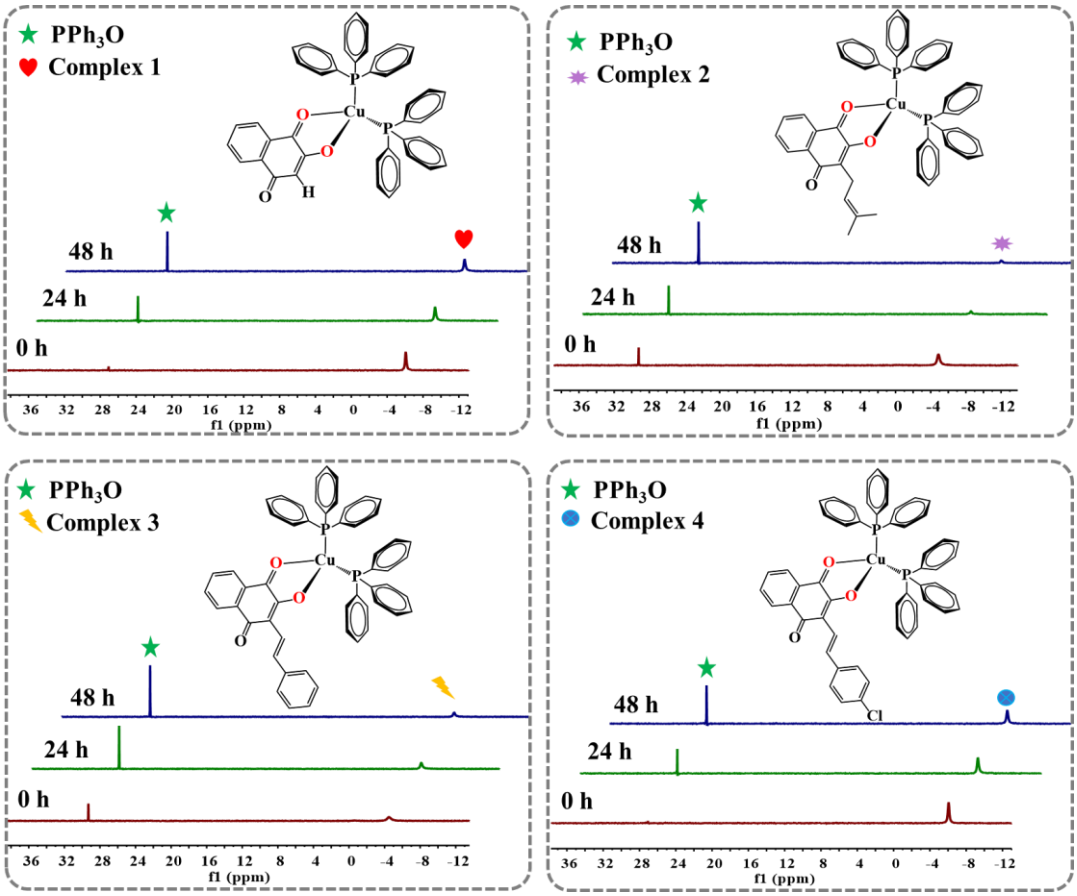

Figure S34. $^{31}P(^{1}H)$ NMR spectra in DMSO/Culture medium 9:1 of the complexes 1, 2, 3, and 4 at different times.

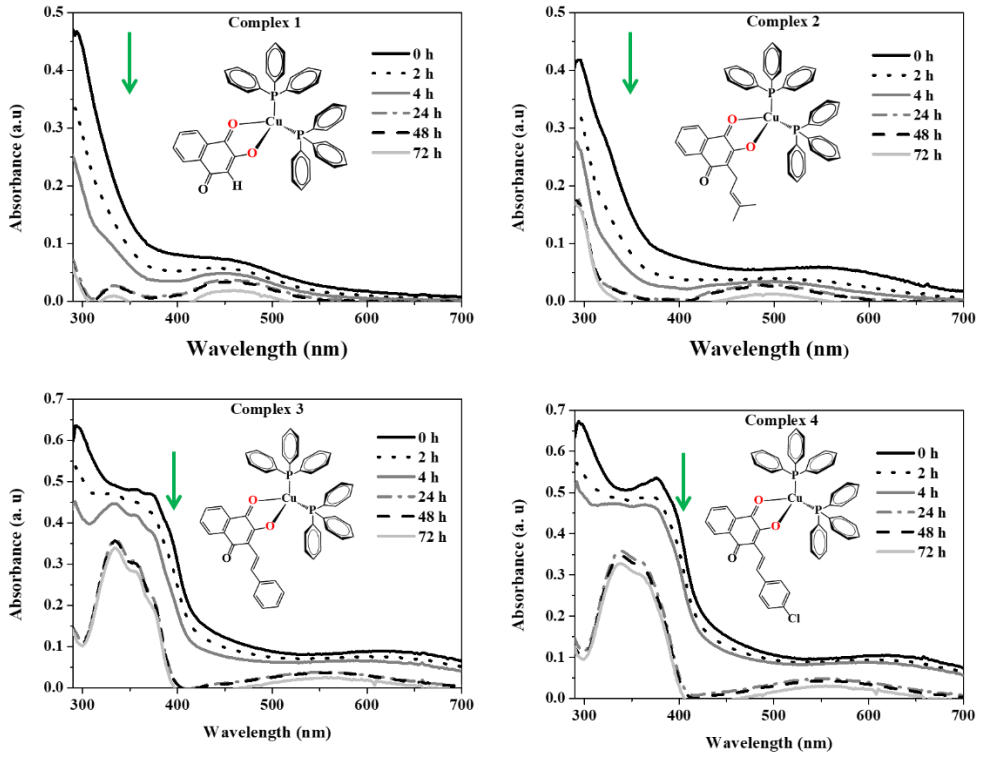

Figure S35. UV-vis spectra in DMSO/Culture medium 1:199 of the complexes 1, 2, 3, and 4 at different times.

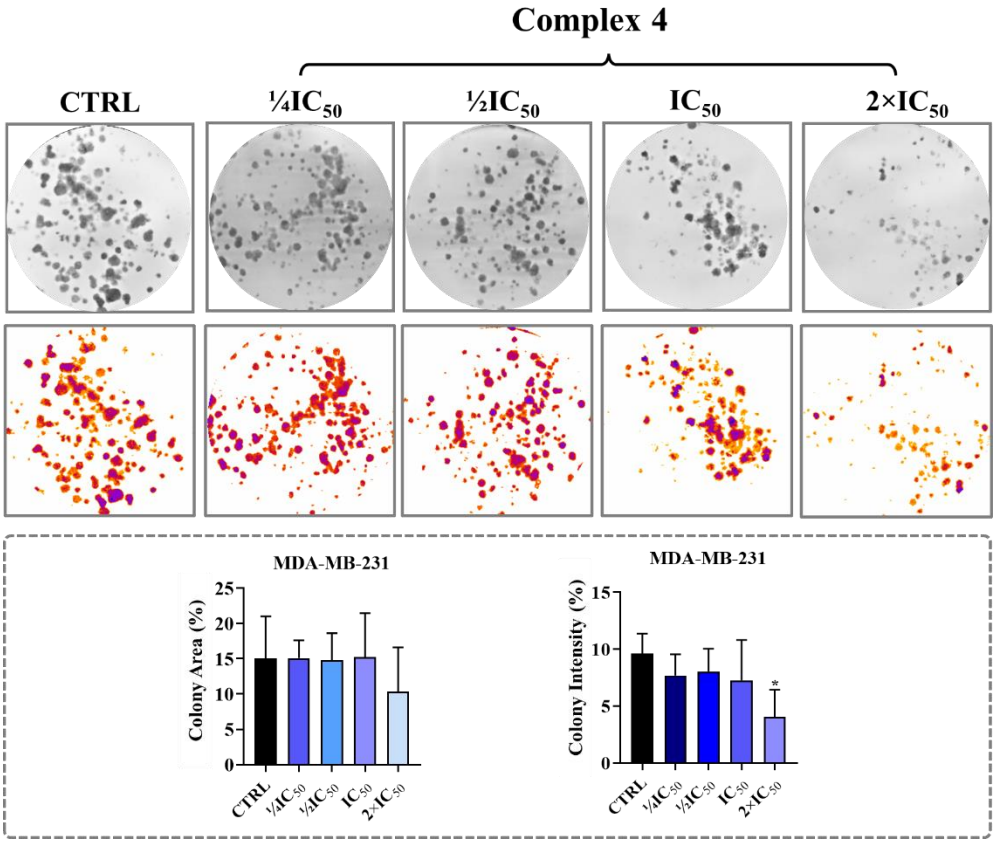

Figure S36. Clonogenic survival of MDA-MB-231 cells treated with different concentrations of complex 4 for 48 h. (a) representation of wells and thresholds for the experiment, and (b) graphical quantifications of colony area and intensity. Data represent the mean ± SD of assays in triplicate. Significance at * $p < 0.05$, ** $p < 0.01$, *** $p < 0.001$, and **** $p < 0.0001$ levels using ANOVA and Dunnet's test.

TABLES

Table S6. Crystal data and structure refinement parameters obtained for the complexes 1and 2.

	1		**2**	
Empirical formula	$C_{46}H_{35}CuO_3P_2$		$C_{51}H_{43}CuO_3P_2$	
Formula weight	761.22 g/ mol		829.33 g/ mol	
Temperature	293(2)K		293(2) K	
Crystal system	Triclinic		Monoclinic	
Space group	P-1		C2/c	
Unit cell dimensions	a = 11.0338(3) Å b = 13.0129(4) Å c = 13.0135(4) Å	α = 81.615(2) ° β = 81.377(2) ° γ = 86.994(2) °	a = 33.7146(7) Å b = 10.3104(2) Å c = 24.1716(5) Å	α = 90° β = 93.374(2)° γ = 90°
Volume	1826.74(9) $Å^3$		8387.8(3) $Å^3$	
Z	2		8	
ρ_{calc}	1.384 g/cm^3		1.313 g/cm^3	
μ	0.728 mm^{-1}		0.640 mm^{-1}	
F (000)	788.0		3456.0	
Crystal size	0.18 × 0.08 × 0.08 mm^3		0.28 × 0.16 × 0.14 mm^3	
2θ range for data collection	5.256 a 61.014 °		5.29 a 55.752°	
Index ranges	$-15 \le h \le 15, -18 \le k \le 18, -18 \le l \le 18$		$-44 \le h \le 44, -13 \le k \le 13, -31 \le l \le 31$	
Reflections collected	51556		82100	
Independent reflections	11133 [R_{int} = 0.0328, R_{sigma} = 0.0261]		10004 [R_{int} = 0.0408, R_{sigma} = 0.0254]	
Data/restraints/parameters	11133/0/469		10004/4/566	
Goodness-of-fit on F^2	1.044		1.060	
Final R indexes [I>=2σ (I)]	R_1 = 0.0348, wR_2 = 0.0821		R_1 = 0.0386, wR_2 = 0.0891	
Final R indexes [all data]	R_1 = 0.0571, wR_2 = 0.0951		R_1 = 0.0605, wR_2 = 0.1031	
Largest diff. peak/hole	0.33/-0.32e.$Å^{-3}$		0.36/-0.34e.$Å^{-3}$	

Table S7. Tentative assignment of the vibrational frequencies (cm^{-1}) of the ν(C1=O1 ν(C2-O2) and ν(C4=O3) stretches for the free and after coordinated naphthoquinone ligands, and the respective shifts (Δ) after coordination.

	Free Ligands (Coordinated Ligands)					
	ν(C1=O1) cm^{-1}	Δ1 (cm^{-1})	ν(C2-O2) cm^{-1}	Δ2 (cm^{-1})	ν(C4=O3) cm^{-1}	Δ3 (cm^{-1})
1	1651(1587)	64	984(1094)	110	1680(1641)	39
2	1639(1583)	56	1047(1095)	48	1663(1628)	35
3	1641(1584)	56	1057(1094)	37	1663(1628)	35
4	1645(1582)	63	1051(1093)	42	1665(1626)	39

Table S8. Maximum absorption wavelength (λ, nm), molar absorptivity (ε, $mol^{-1}L\ cm^{-1}$), and tentative assignment of the bands of the ligands NQ1 NQ4 and their respective complexes 1-4 in acetonitrile solution.

Ligands	**λ (nm)**	**ε ($mol^{-1}Lcm^{-1}$)**	**Electronic transition**	**Complexes**	**λ (nm)**	**ε ($mol^{-1}Lcm^{-1}$)**	**Electronic transition**
NQ1	250	19741	π→π*	**1**	276	35247	ILCT/ MLCT
	276	18776	π→π*		330	Ombro	ILCT: n→π*
	332	3362	n→π*/ICT		488	3057	ICT
NQ2	254	28331	π→π*	**2**	254	42709	ILCT
	284	18886	π→π*		274	37521	ILCT/ MLCT
	334	3937	n→π*/ICT		330	Ombro	n→π*
					540	3856	ICT
NQ3	236	15489	π→π*	**3**	266	38150	ILCT/ MLCT
	310	36810	π→π*		334	17200	ILCT
	462	7230	n→π*		376	30405	ICT
					582	3408	ILCT: n→π*
NQ4	228	23120	π→π*	**4**	264	40408	ILCT/ MLCT
	312	53120	π→π*		334	16505	ILCT
	462	10573	n→π*		382	35268	ICT
					510	3537	ILCT: n→π*

Table S9. EPR parameters obtained from simulation of the experimental spectra of the DMPO-˙OOH and DMPO-˙OH adducts.

EPR parameters		
	DMPO-˙OOH	DMPO-˙OH
$\mathbf{g_0}$	2.0060	2.0059
lwpp1	[0.0835 0.0743] mT	[0.1387 0.0456] mT
A_N	36.16 MHz (1.297 mT)	38.89 MHz (1.395 mT)
A_{H1}	29.37 MHz (1.053 mT)	32.93 MHz (1.181 mT)
A_{H2}	3.71 MHz (0.133 mT)	

Table S10. EPR parameters obtained from simulation of the spectrum measured at 77K temperature (liquid N2), with four spectral components.

Component	g[x y z]	A_{Cu}[x y z]	A_P[x y z]	Q_{Cu}[Q n]	Lw[x y z]
C1	2.0400 2.0400 2.3055	90.0 90.0 505.0	30.0 30.0 10.0	20.0 -10.0	25.0 25.0 25.0
C2	2.0825 2.0634 2.3170	30.0 50.0 490.0	30.0 30.0 10.0	10.0 9.0	20.0 20.0 20.0
C3	2.0270 2.0740 2.2743	90.0 20.0 540.0	- -	18.0 -11.0	20.0 20.0 40.0
C4	2.0800 2.0800 2.2410	30.0 30.0 555.0	- -	22.0 10.0	40.0 40.0 60.0

Os valores de A_{Cu}, A_P, Q_{Cu}, Lw estão dados em MHz.